

# Entropy generation in peristaltic pumping of viscoplastic fluids through a planar channel : A comparative study

H. RACHID<sup>a 1</sup>, M. OUAZZANI TOUHAMI<sup>a</sup>, N. LAHLOU<sup>a</sup>

a. Laboratory of Mechanics, Faculty of Science Ain Chock, University Hassan II, Casablanca, Morocco

## Résumé :

*Dans ce papier, nous avons étudié le transport péristaltique de fluids viscoplastiques à trois paramètres en présence du transfert de chaleur dans un canal plan. Le deuxième principe de thermodynamique a été utilisé pour déterminer la génération d'entropie du système. Nous avons déterminé les solutions analytiques dans le cas des grandes longueurs d'onde et faible nombre de Reynolds. Les effets des paramètres physiques du problème sur le profile de vitesse, le rapport la force de frottement/chute de pression, l'efficacité mécanique, le profile de temperature, l'entropie et sur le nombre de Bejan ont été mis en évidence. De plus, une comparaison des résultats a été faite entre le modèle de Herschel-Bulkley et le modèle de Vocadlo d'une part et par rapport aux fluides : Newtonian, à loi puissance et de Bingham, d'autre part.*

## Abstract :

*In this paper we studied the peristaltic pumping of three-parameters viscoplastic fluids with heat transfer through a planar channel. The second law of thermodynamics is used to determine to entropy generation of the system. The closed solutions of the problem are obtained in the case of long wavelength and low Reynolds number approximations. The effects of embedded parameters on the velocity, ratio frictional force/pressure rise, mechanical efficiency, temperature, entropy generation and on the Bejan number have been analyzed through graphs. In addition, the comparisons of the results between the Herschel-Bulkley and Vocadlo models or versus a Newtonian, power-law and Bingham fluids have been made.*

**Keywords : Peristaltic pumping / Three-parameter plastic fluids/ Entropy generation/ Mechanical efficiency/ Bejan number/ planar channel**

## 1 Introduction

Non-Newtonian viscoplastic (or yield stress) fluids are materials that behaves like a rigid solid body when a small shear stress is applied. Once the yield stress exceeds a certain critical value  $\tau_0$  then the materiel deforms and flows as a viscous fluid. Practically, such fluid flow appears in many industrial

1. Corresponding author : rhassan2@yahoo.fr

processes, as in the food industry (Ketchup, mayonnaise, chocolate,...), the petroleum industry (drilling mud, cement, waxy crude oil,...), the biological industry (mucus, blood clot,...), the natural phenomena (flows of slurries, debris and lava,...), and in various complex printing and coating processes. The two-parameter Bingham fluid was the first studied model and in different geometries as in [1]. Later, the researchers proposed three-parameter viscoplastic models such as the Herschel-Bulkley [2], Casson [3] or Vocadlo (sometimes called Robertson-Stiff one) [4] fluids, etc. The peristaltic transport is one of the major application of fluide-structure interaction phenomenon. Many researchers studied this type of transport for a Newtonian or non-Newtonian fluids as in [5–7]. The flow of blood or of the food bolus in the human body, the transportation of high-viscosity fluids and solid-liquid mixtures, include cement plants, sewage treatment plants, sanitary fluid and food plants are some physiological and industrial applications of peristalsis. The impact of heat transfer on fluid flow plays an important role in industry or in mechanical engineering, this importance attracted many researchers to study this coupling in recent years. For example, hayat *et al.* [8] investigated the peristaltic pumping of a Newtonian fluid with heat transfer and slip conditions in an asymmetric channel. Akbar *et al.* [9] studied the heat transfer analysis of Rabinowitsch fluid flow due to metachronal wave of cilia in circular cylindrical tube. The Electromagnetohydrodynamic (EMHD) flow with heat transfer on third-grade fluid containing small particles has been investigated by Bhatti *et al.* [10]. In 1865, Clausius [11] introduced a state function called "entropy" which characterize an extensive property of the system and it define the irreversibility, the degree of system disorganization and to upgrade the system performance. Because of the importance of this physical quantity in heat transfer phenomenon, some researchers applied the second law of thermodynamics to study the entropy in several physical situations. Abolbashari *et al.* [12] analyzed a Casson nano-fluid flow induced by a stretching surface with velocity slip and convective surface boundary condition. The entropy generation in stagnation point flow of non-Newtonian Jeffrey, Maxwell, and Oldroyd-B nanofluids along a linear porous stretching sheet has been studied by Almakki *et al.* [13].

Experimentally, Beirute and Flumerfelt [14] presented a comparative data (for cement slurry along with fitting curves) between the two proposed fluids. The authors found that the Vocadlo (or RS) model is somewhat superior and they proposed it as an improved one for cement slurries even for different cement slurry of higher yield.

In this article, we present a comparative study of the peristaltic pumping between the Herschel-Bulkley and the Vocadlo models in the presence of heat transfer through a deformable planar channel with a sinusoidal wave traveling down its walls. The axial velocity profile, the ratio frictional force/pressure rise, mechanical efficiency, temperature profile, entropy generation and the Bejan number have been analyzed versus the physical parameters (the power index of fluid  $n$ , the yield stress or the threshold  $\tau$ , the Brinkman number  $Br$  and the occlusion  $\phi$ ) through graphs. Also, these results have been compared with those of a Newtonian, power-law and Bingham models.

## 2 Formulation and analysis

We consider a steady peristaltic flow of incompressible Herschel-Bulkley (HB) and Vocadlo (V) fluids with heat transfer in a symmetric planar channel.

In the fixed frame  $(\bar{X}, \bar{Y})$  the equations of the walls are :  $\bar{H} = a + b \sin \frac{2\pi}{\lambda}(\bar{X} - c\bar{t})$ .

The constitutive equations of the fluids are written as follows :  $\bar{\tau}_{(HB)} = (\bar{\tau}_0 + \mu \bar{\gamma}^n)$  ;  $\bar{\tau}_{(V)} = (\bar{\tau}_0 + \mu \bar{\gamma})^n$

If we introduce the following non-dimensional quantities :

$$x = \frac{\bar{x}}{\lambda}; y = \frac{\bar{y}}{a}; t = \frac{c\bar{t}}{\lambda}; u = \frac{\bar{u}}{c}; v = \frac{\bar{v}}{\varepsilon c}; p = \frac{\bar{p}}{\frac{\mu\lambda c^n}{a^{n+1}}}; \dot{\gamma} = \frac{\bar{\dot{\gamma}}}{\left(\frac{c}{a}\right)}; \tau = \frac{\bar{\tau}}{\mu\left(\frac{c}{a}\right)^n}; \tau_0 = \frac{\bar{\tau}_0}{\mu\left(\frac{c}{a}\right)^n}; Q = \frac{\bar{Q}}{ac};$$

$$\theta = \frac{\bar{T} - T_w}{T_0 - T_w}; \phi = \frac{b}{a}; \varepsilon = \frac{a}{\lambda}; Re = \frac{\rho a^n}{\mu c^{n-2}}; Pr = \frac{\mu c_p}{k}; Ec = \frac{c^2}{c_p(\bar{T}_0 - \bar{T}_1)}; \Omega = \frac{(T_0 - T_w)^2}{T_0^2} \quad (1)$$

$\varepsilon$ ,  $Re$ ,  $Pr$ ,  $Ec$  and  $Br = Pr Ec$  are the wave, Reynolds, Prandtl, Eckert and the Brinkman numbers, respectively.  $\phi$  is the amplitude ratio with  $0 < \phi < 1$ .

In order to solve our problem analytically, we suppose that  $\varepsilon \ll 1$  (long wavelength) and  $Re \ll 1$  (low Reynolds number). In this case, we find (in the wave frame) the following non-dimensional equations :

$$\frac{\partial u}{\partial x} + \frac{\partial v}{\partial y} = 0 \quad (2)$$

$$\frac{\partial p}{\partial y} = 0 \quad (3)$$

$$-\frac{\partial p}{\partial x} = \left(\frac{\partial \tau_{xy}}{\partial y}\right) \quad (4)$$

$$Br \left( \tau_{xy} \frac{\partial u}{\partial y} \right) + \left( \frac{\partial^2 \theta}{\partial y^2} \right) = 0 \quad (5)$$

$$\tau_{(HB)} = (\tau_0 + \dot{\gamma}^n) \quad (6)$$

$$\tau_{(V)} = (\tau_0 + \dot{\gamma})^n \quad (7)$$

$$\frac{\partial u}{\partial y}(y=0) = 0 ; u(y=H) = -1; \quad (8)$$

$$\frac{\partial \theta}{\partial y}(y=0) = 0 ; \theta(y=H) = 0 \quad (9)$$

The solutions of (2-9) are given by :

In the non-plug region ( $r_0 \leq r \leq H$ ) :

$$u_{(HB)} = -\frac{n}{n+1}(-\mathbf{A})^{\frac{1}{n}} \left[ (\mathbf{y} - \tau)^{\frac{n+1}{n}} - (\mathbf{H} - \tau)^{\frac{n+1}{n}} \right] - 1 \quad (10)$$

$$u_{(V)} = -\frac{n}{n+1}(-\mathbf{A})^{\frac{1}{n}} \left[ (\mathbf{y}^{\frac{n+1}{n}} - \mathbf{H}^{\frac{n+1}{n}}) - \frac{\mathbf{n}+1}{\mathbf{n}} \tau^{\frac{1}{n}} (\mathbf{y} - \mathbf{H}) \right] - 1 \quad (11)$$

$$\theta_{(HB)} = Br(-\mathbf{A})^{\frac{n+1}{n}} \left( \int_{\mathbf{H}}^{\mathbf{y}} \int_0^{\xi} \eta(\eta - \tau)^{\frac{1}{n}} d\eta d\xi \right) \quad (12)$$

$$\theta_{(V)} = Br(-\mathbf{A})^{\frac{n+1}{n}} \left( \int_{\mathbf{H}}^{\mathbf{y}} \int_0^{\xi} \eta(\eta^{\frac{1}{n}} - \tau^{\frac{1}{n}}) d\eta d\xi \right) \quad (13)$$

- In the plug region ( $0 \leq r \leq r_0$ ) :

$$up = u(y = \tau H) ; \theta p = \theta(y = \tau H) \quad (14)$$

with  $\mathbf{A} = \frac{\partial \mathbf{p}}{\partial \mathbf{x}}$  and  $\tau = \frac{y_0}{H} = \frac{\tau_0}{\tau_H}$  (say).

The volume flow rate in the moving frame is :  $q = \int_0^{y_0} u_p dy + \int_{y_0}^H u dy$ .

using the following changes :  $y = Y$ ;  $x = X - t$ ;  $p = P$ ;  $u(x, y) = U(X - t, Y) - 1$ ;

$v(x, y) = V(X - t, Y)$ ,  $q = Q - H$  and from the flow rate and the velocity expressions we find the expression of the pressure gradient as follows :

$$\frac{\partial p}{\partial x (HB)} = (-1)^{n+1} \left( \frac{n+1}{n} \right)^n \frac{(Q + H - 1)^n}{(a1 + a2 + a3)^n} \quad (15)$$

$$\frac{\partial p}{\partial x (V)} = (-1)^{n+1} \left( \frac{n+1}{n} \right)^n \frac{(Q + H - 1)^n}{((b1 + b2) + \frac{n+1}{n}(b3 + b4))^n} \quad (16)$$

with :  $a1 = - \int_0^{y_0} (H - y_0)^{\frac{n+1}{n}} dy$  ;  $a2 = - \int_{y_0}^H (H - y_0)^{\frac{n+1}{n}} dy$  ;  $a3 = \int_{y_0}^H (y - y_0)^{\frac{n+1}{n}} dy$  ;  
 $b1 = \int_0^{y_0} (y_0^{\frac{n+1}{n}} - H^{\frac{n+1}{n}}) dy$  ;  $b2 = \int_{y_0}^H (y^{\frac{n+1}{n}} - H^{\frac{n+1}{n}}) dy$  ;  $b3 = - \int_0^{y_0} y_0^{\frac{1}{n}} (y_0 - H) dy$  ;  
 $b4 = - \int_{y_0}^H y_0^{\frac{1}{n}} (y - H) dy$

The non-dimensional pressure rise and frictional force over a wavelength can be found through the relations :

$$\Delta p = \int_0^1 \frac{\partial p}{\partial x} dx \quad ; \quad F = - \int_0^1 H \frac{\partial p}{\partial x} dx \quad (17)$$

The dimensionless mechanical efficiency of pumping is given by :

$$E = \frac{Q \Delta p}{\Delta p H_{(x=0)} + F} = \frac{1}{1 + \frac{F}{\Delta p}} \quad (18)$$

with  $H_{(x=0)} = 1$ .

The entropy generation  $\dot{S}_g$  rate of a non-Newtonian fluid can be written as [15] :

$$\dot{S}_g = \dot{S}_{(HT)} + \dot{S}_{(FF)} = \frac{k}{T_0^2} \left( \left( \frac{\partial \bar{T}}{\partial x} \right)^2 + \left( \frac{\partial \bar{T}}{\partial y} \right)^2 \right) \frac{1}{T_0} \left( \bar{\tau}_{xx} \frac{\partial \bar{u}}{\partial x} + \bar{\tau}_{yy} \frac{\partial \bar{v}}{\partial y} + \bar{\tau}_{xy} \left( \frac{\partial \bar{v}}{\partial x} + \frac{\partial \bar{u}}{\partial y} \right) \right) \quad (19)$$

where  $\dot{S}_{(HT)}$  and  $\dot{S}_{(FF)}$  are the heat transfer entropy generation and the friction dissipation entropy generation, respectively. If we consider the following dimensionless entropy generation  $N_s = \frac{\dot{S}_g}{\frac{k(T_0 - T_1)^2}{a^2 T_0^2}}$

and under the approximations of the problem, the Eq. (19) becomes :

$$N_s = N_{s(HT)} + N_{s(FF)} = \left( \frac{\partial \theta}{\partial y} \right)^2 + \frac{Br}{\Omega} \tau_{xy} \frac{\partial u}{\partial y} \quad (20)$$

The Bejan number is defined as the ratio of heat transfer entropy generation  $N_{sHT}$  to total entropy generation rate  $N_s$ , it is given by :

$$Be = \frac{N_{s(HT)}}{N_s} = \frac{\left( \frac{\partial \theta}{\partial y} \right)^2}{N_s} = \frac{1}{1 + \chi} \quad (21)$$

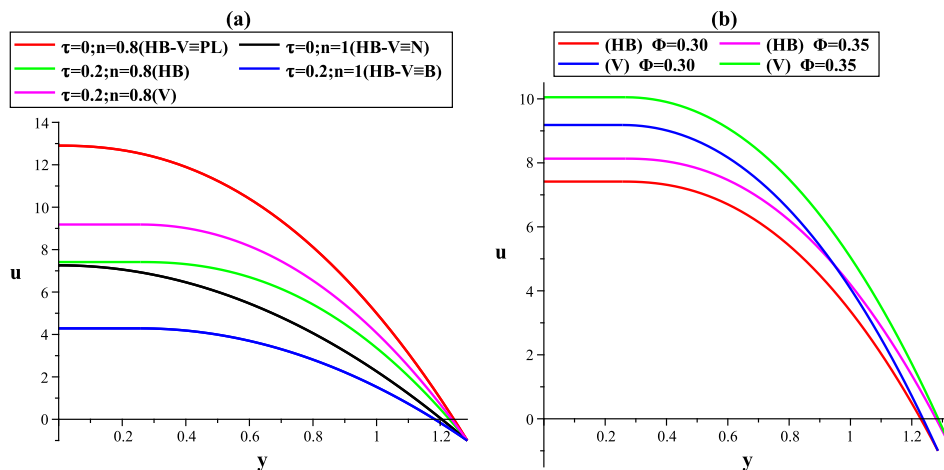


FIGURE 1 – Velocity profile for  $\frac{\partial p}{\partial z} = -10$  and  $z = 0.2$  (a) effects of  $n$  and  $\tau$  for  $\phi = 0.3$  (b) effect of  $\phi$  for  $n = 0.8$  and  $\tau = 0.2$ .

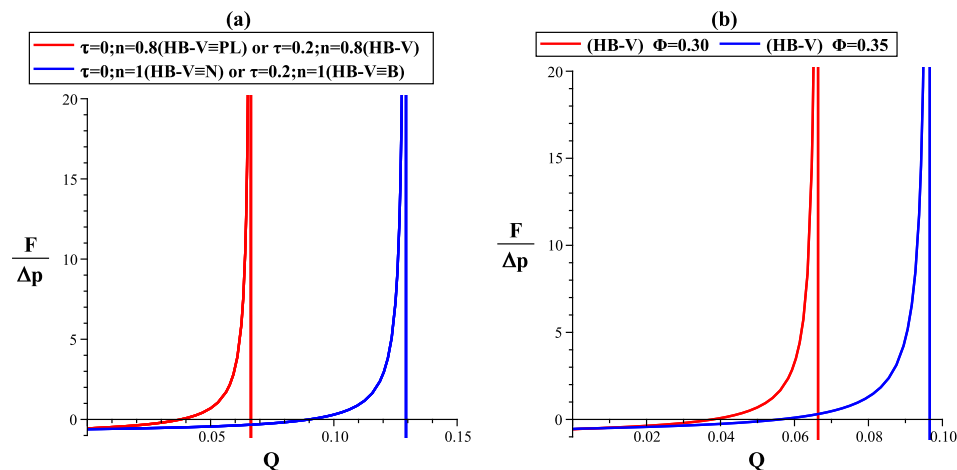


FIGURE 2 – The ratio  $\frac{F}{\Delta p}$  versus  $Q$  (a) effects of  $n$  and  $\tau$  for  $\phi = 0.3$  (b) effect of  $\phi$  for  $n = 0.8$  and  $\tau = 0.2$ .

with  $\chi = \frac{Ns_{(FF)}}{Ns_{(HT)}}$  is the irreversibility ratio.

### 3 Results and discussion

The effects of embedded parameters on physical quantities of problem have been analyzed through graphs in this section. Before, we notice that when  $n = 1$  and  $\tau \neq 0$ ;  $n \neq 1$  and  $\tau = 0$ ;  $n = 1$  and  $\tau = 0$  we find the Bingham, power-law and the Newtonian models, respectively. Figure (1) show that the axial velocity increases with increasing the occlusion  $\phi$  while it decreases with increasing the flow index number  $n$  and the yield stress threshold  $\tau$ . In addition, the velocity of the proposed models (HB and V) is bigger than that of the Bingham fluid and smaller than that of the power-law model. Also, the flow for the Vocadlo model is faster when compared to the Herschel-Bulkley model. Maybe for this reason, Beirute and Flumerfelt [14] proposed the Vocadlo (or so-called Robetson-Stiff) model as an improved model for cement slurries. In order to analyze the variations of mechanical efficiency  $E$ , we plot in Figure (2) the ratio  $\frac{F}{\Delta p}$  (see Eq. (18)). First, when  $Q = 0$  or  $\Delta p = 0$  or both, we observe that  $E = 0$ . Second, when  $Q \neq 0$  and  $\Delta p \neq 0$ , we have three cases :

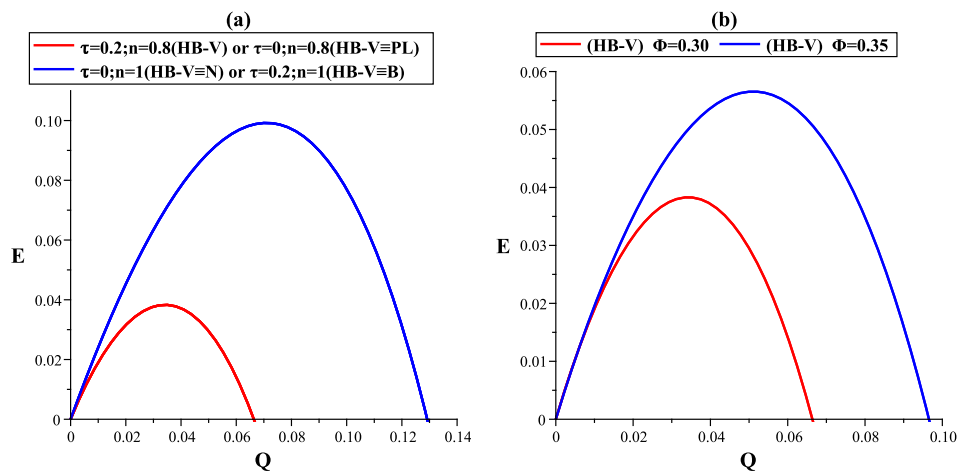


FIGURE 3 – Mechanical efficiency  $E$  versus  $Q$  (a) effects of  $n$  and  $\tau$  for  $\phi = 0.3$  (b) effect of  $\phi$  for  $n = 0.8$  and  $\tau = 0.2$ .

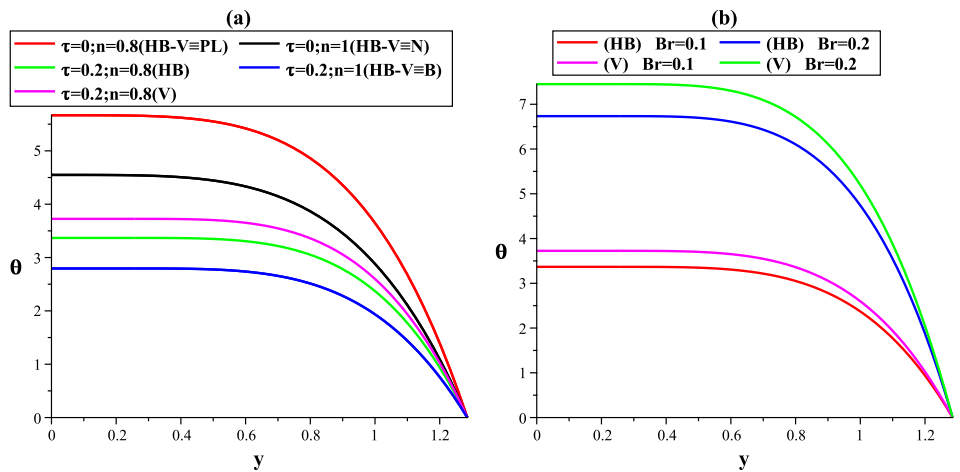


FIGURE 4 – Temperature profile  $\theta$  for  $\phi = 0.3$ ,  $\frac{\partial p}{\partial z} = -10$  and  $z = 0.2$  and  $\Omega = 0.5$  (a) effects of  $n$  and  $\tau$  for  $Br = 0.1$  (b) effect of  $Br$  for  $n = 0.9$  and  $\tau = 0.2$ .

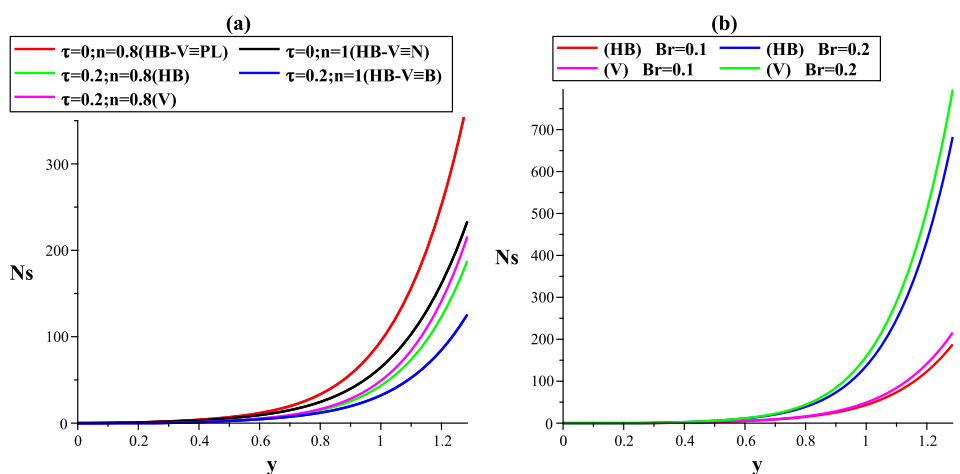


FIGURE 5 – Entropy generation rate  $Ns$  for  $\phi = 0.3$ ,  $\frac{\partial p}{\partial z} = -10$  and  $z = 0.2$  and  $\Omega = 0.5$  (a) effects of  $n$  and  $\tau$  for  $Br = 0.1$  (b) effect of  $Br$  for  $n = 0.9$  and  $\tau = 0.2$ .

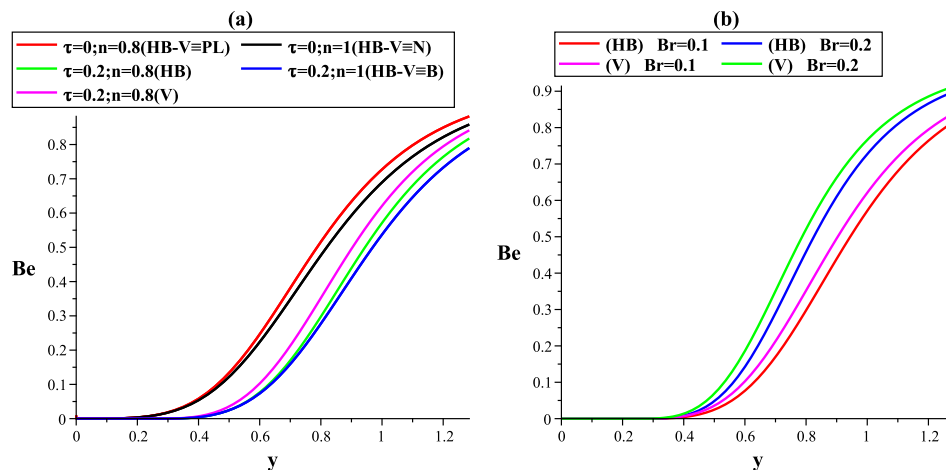


FIGURE 6 – Bejan number  $Be$  for  $\phi = 0.3$ ,  $\frac{\partial p}{\partial z} = -10$  and  $z = 0.2$  and  $\Omega = 0.5$  (a) effects of  $n$  and  $\tau$  for  $Br = 0.1$  (b) effect of  $Br$  for  $n = 0.9$  and  $\tau = 0.2$ .

Case1 : When  $\frac{F}{\Delta p} < 0$ , this ratio slowly increases versus the time-averaged flow rate  $Q$  i.e, the mechanical efficiency increases with the increase in  $Q$  (see Figure (3)).

Case2 : When  $\frac{F}{\Delta p} > 0$ , a rapid increase of the ratio versus  $Q$  is observed i.e,  $Q$  reduces the mechanical efficiency  $E$ .

Case3 : For  $\frac{F}{\Delta p} = 0$ ,  $E$  becomes maximum and we have  $E = Q$  (see Eq. (18)).

Third, Figure (2) also shows that there is no difference between the vocadlo, the Herschel-Bulkley and the power-law models or between the Bingham and the Newtonian models i.e, there is no effect of the yield stress threshold  $\tau$  on  $\frac{F}{\Delta p}$  and then on mechanical efficiency. The flow index  $n$  enhances the pumping  $Q$  and then  $E$  for a given value of the ratio  $\frac{F}{\Delta p}$  when we compare the power-law with the Newtonian model or the Herschel-Bulkley and the vocadlo with the Bingham fluid. Firth, the pumping  $Q$  and the mechanical efficiency increase with increasing the occlusion  $\phi$ . In Figures (4-6) we present the temperature profile  $\theta$ , the entropy generation rate  $Ns$  and the Bejan number  $Be$ , respectively. It is seen that these quantities have the same variations versus the physical parameters i.e, they decrease with an increase in  $n$  and  $\tau$  while they increase with increasing the Brinkman number  $Br$ . In addition, they are bigger for the vocadlo model than the Herschel-Bulkley model. Physically,  $Br$  has accelerating effect on the temperature profile and it is proposed as a parameter for correlating the convective heat transfer parameters in microchannels. It also indicates the presence of heat transfer induced by variations of viscosity and flow velocity and the fact that  $Br$  incorporates viscous dissipation effects which expands the fluid temperature. On the other hand, low values of  $Br$  or higher values of  $n$  and  $\tau$  are required to minimize the entropy generation (i.e, the irreversibility) and then a better working performance of the system.

## 4 Conclusion

The present study investigates the coupling between peristaltic pumping and heat transfer of three-parameters viscoplastic fluids in a symmetric planar channel. The effects of physical parameters on velocity, mechanical efficiency, temperature, entropy generation and on Bejan number have been discussed through graphs. The comparisons between the vocadlo and the Herschell-Bulkley models (on one

hand) or between these models and the power-law, Bingham or the Newtonian fluids (on other hand) have been analyzed. It is observed that the all physical quantities are higher for the vocadlo model when compared to the Herschel-Bulkley model except the mechanical efficiency which remain the same for the two models. The quantities for both models are bigger than those of the Bingham fluid and smaller than those of the power-law model.

## Références

- [1] K. F. Liu, C. C. Mei, Slow spreading of a sheet of Bingham fluid on an inclined plane, *Journal of Fluid Mechanics*, 207 (1989) 505–529.
- [2] J. D. Sherwood, D. Durban, Squeeze-flow of a Herschel-Bulkley fluid, *Journal of non-Newtonian Fluid Mechanics*, 77 (1998) 115–121.
- [3] F. Mabood, K. Das, Outlining the impact of melting on MHD Casson fluid flow past a stretching sheet in a porous medium with radiation, *Heliyon*, 5 (2019) e01216.
- [4] J. J. Vocadlo, M. E. Charles, Characterization and laminar flow of fluid like viscoplastic substances, *The Canadian Journal of Chemical Engineering*, 31 (1973) 116–121.
- [5] J. B. Shukla, R. S. Parihar, B. R. P. Rao, S. P. Gupta, Effects of peripheral-layer viscosity on peristaltic transport of a bio-fluid, *Journal of Fluid Mechanics*, 97 (1980) 225–237.
- [6] H. Rachid, M. T. Ouazzani, Interaction of pulsatile flow with peristaltic transport of a viscoelastic fluid : case of a Maxwell fluid, *International Journal of Applied Mechanics*, 6 (2014) 1450061.
- [7] N. Ali, K. Ullah, Bifurcation analysis for peristaltic transport of a power-law fluid, *Zeitschrift für Naturforschung A*, 74 (2019) 213.
- [8] T. Hayat, S. Hina, N. Ali, Simultaneous effects of slip and heat transfer on the peristaltic flow, *Communications in Nonlinear Science and Numerical Simulation*, 15 (2010) 1526–1537.
- [9] N. S. Akbar, A. W. Butt, Heat transfer analysis of Rabinowitsch fluid flow due to metachronal wave of cilia, *Results in Physics*, 5 (2015) 92–98.
- [10] M.M. Bhatti, A. Zeeshan, R. Ellahi, Electromagnetohydrodynamic (EMHD) peristaltic flow of solid particles in a third-grade fluid with heat transfer, *Mechanics & Industry*, 18 (2017) 314–322.
- [11] R. Clausius, Ueber verschiedene für die Anwendung bequeme Formen der Hauptgleichungen der mechanischen Wärmetheorie, *Annalen der Physik*, 201 (1865) 353–400.
- [12] M. H. Abolbashari, N. Freidoonimehr, F. Nazari, M. Mehdi Rashidi, Analytical modeling of entropy generation for Casson nano-fluid flow induced by a stretching surface, *Advanced Powder Technology*, 26 (2015) 542–552.
- [13] M. Almakki, S. K. Nandy, S. Mondal, P. Sibanda, D. Sibanda, A model for entropy generation in stagnationpoint flow of non-Newtonian Jeffrey, Maxwell, and Oldroyd-B nanofluids, *Heat Transfer-Asian Research*, 48 (2019) 24–41.
- [14] R. M. Beirute, R. W. Flumerfelt, An evaluation of the Robertson-Stiff model describing rheological properties of drilling fluids and cement slurries, *Society of Petroleum Engineers*, 17 (1977) 97–100.
- [15] A. Bejan, *Entropy generation through heat and fluid flow*, Wiley, New York, 1982.